Volume 3, Number 2, 2010. pp. 61-68

Jordan Journal of Physics

ARTICLE

# AFM Study of Multilayer Sol-gel $Ba_xSr_{1-x}TiO_3$ Thin Films

**Ala'eddin A. Saif, N. Ramli** and **P. Poopalan**

*Microfabrication Cleanroom, School of Microelectronic Engineering, University Malaysia Perlis (UniMAP), Kuala Perlis, 02000, Perlis, Malaysia.*

*Received on: 15/3/2010; Accepted on: 5/9/2010*

**Abstract:** Multilayer Barium Strontium Titanate (BST) sol-gel films with molar formula $Ba_xSr_{1-x}TiO_3$ ($x$ = 0.5, 0.7 and 0.8) are deposited on $SiO_2$/Si substrates. The surface morphology and grain size are characterized via Atomic Force Microscope (AFM), showing the films to be uniform and crack-free. The average roughness, maximum peak to valley height, root mean square (RMS) roughness, ten-point mean height roughness, surface skewness and surface kurtosis parameters are used to analyze the surface morphology of the BST thin films. Generally, the results show that the surface roughness increases with decreasing Sr content with RMS roughness increasing from 4.77 nm to 6.52 nm for films of 160.8 nm thickness as Sr content decreases. Surface roughness also increases with the film thickness, for $x$ = 0.5, RMS roughness increases from 4.77 nm to 13.33 nm as the film thickness increases from 160.8 nm to 446.8 nm. A similar trend for surface roughness is obtained, for all $x$ values, as is for grain size.
**Keywords:** BST; Thin film; Sol-gel; AFM; Surface roughness.
**PACS**: 68.37.Ps; 68.55.J-; 81.20.Fw; 77.55.fe.

## Introduction

Ferroelectric Barium Strontium Titanate (BST) thin films have been widely investigated as a potential material for use in microelectronic devices such as non-volatile random access memory (RAM) and ferroelectric field effect transistor (FeFET) due to its high dielectric constant, as well as relatively low dielectric loss tangent. Furthermore, its desirable pyroelectric and piezoelectric properties can be utilized for a variety of sensing applications [1, 2]. Therefore, a large number of studies have been conducted to improve the quality of BST thin films. An important factor in all the applications of BST is its surface structure. Hence, it is imperative to have a good understanding of the surface morphology of BST thin films for fabrication of advanced microelectronics devices [3].

Surface morphology plays an important role in various areas of science and technology [4]. It can be used to understand many fundamental problems such as friction, contact deformation, heat and electric current conduction [5]. There are many parameters used to evaluate the surface roughness. These parameters are categorized into three groups: amplitude, spatial and hybrid parameters; however, the most important group is the amplitude parameters [6].

Relatively few studies have focused on the surface roughness of BST thin films. C. Fu *et al.* showed that the grain size and surface roughness increase as the annealing temperature increases [7]. Wencheng Hu *et al.* reported that BST film surface roughness increases with the concentration of precursor solutions [8]. In this work, BST thin films of different Ba:Sr content and different film thicknesses are prepared by the sol-gel technique, and the surface roughness and the grain sizes for these films are determined

**Corresponding Author:** Ala'eddin A. Saif. **Email**: alasaif82@hotmail.com

using an atomic force microscope (AFM). A comprehensive analysis of the BST surface properties using parameters such as the average roughness, maximum peak to valley height, root mean square roughness, ten-point mean height roughness, surface skewness and surface kurtosis is made. These are parameters that allow insight into the surface properties and quality.

## BST Films Preparation

Different values of Ba:Sr content, x, of the $Ba_xSr_{1-x}TiO_3$ solutions were prepared by sol-gel method. Barium acetate, strontium acetate and titanium (IV) isopropoxide were used as starting materials, with glacial acetic acid and 2-Methoxyethanol as solvents. Specific amounts of barium acetate and strontium acetate were dissolved in 10 ml heated acetic acid to obtain the Ba-Sr solution. A stoichiometric amount of titanium (IV) isopropoxide was added to 4ml 2-Methoxyethanol to get a separate solution. Both solutions were then mixed and refluxed separately with the Ba-Sr solution being drip-added to the titanium solution. The final mixture was magnetically stirred at 400 rpm for two hours and refluxed to get a thick solution, which was filtered using a nylon microfiber filter. Three different solutions with Ba:Sr proportions of 50:50, 70:30 and 80:20 were prepared, and labeled BST50, BST70 and BST80, respectively.

BST thin films were spun layer by layer on $SiO_2$/Si substrates with a specific heating procedure. For each layer, the as-deposited BST thin film was baked at 200 °C for 20 min to vaporize the organic solvents. Then, it was heated at 500 °C for 30 min in an $O_2$ atmosphere before the next layer was spun-on. This process was repeated until four layers were deposited. Finally, the BST films were annealed at 800 °C for 1 h in an $O_2$ atmosphere. Films with one, two, three and four layers for each Ba:Sr ratio were prepared with the same procedure.

## Measuring Method

The AFM (SPA400, SII Nanotechnology, Inc.) was operated in contact mode, with a 2.9 μm high tip, less than 20 μm in radius and with a cone angle less than 70°. There are two cantilevers, denoted as A and B, with individual parameters as summarized in Table 1. In contact mode scanning, the low spring constant of the cantilever, which is less than the effective spring constant holding the atoms of the sample together, allows the tip to trace across the sample gently providing high resolution image of the surface compared to tapping mode.

TABLE 1. The dimensions and the mechanical properties of the cantilevers used.

| | Cantilever A | Cantilever B |
|---|---|---|
| Length (L/μm) | 200 | 100 |
| Width (W/μm) | 166 (base) to 6 (head) | 106 (base) to 6 (head) |
| Thickness (t/μm) | 0.4 | 0.4 |
| Resonance frequency (kHz) | 11 | 34 |
| Spring constant (N/m) | 0.02 | 0.08 |

In order to completely characterize the surface, at least 3 images, with an area of 10 μm × 10 μm using cantilever A and scanned at 2 Hz, were recorded for different positions to avoid the edge effect. However, for grain size investigation, the measurement area was reduced to 500 nm × 500 nm with cantilever B and a 2 Hz scan speed. Specific roughness parameters were extracted using Gwyddion software [9].

In order to measure the film thickness, the films were partially dipped in diluted hydrofluoric acid (HF); the resulting step-profile thickness was measured with a stylus profilometer. The thicknesses of one, two, three and four layers of BST50 films were: 149.5 nm, 226.6 nm, 356.8 nm and 435.2 nm, respectively, and for BST70 films: 160.8 nm, 235.6 nm, 368.5 nm and 446.8 nm, respectively, and for BST80 films: 165.4 nm, 247.1 nm, 374.6 nm and 449.3 nm, respectively. However, the BST70 values were taken as the reference benchmark for all of the BST ratios in this article.

### AFM Amplitude Analysis

The amplitude parameters of a sample are described by parameters which give information about statistical average values, shape of the histogram heights and other extreme properties.

The average roughness ($R_a$) is the mean height as calculated over the entire measured length/area. Maximum peak to valley height roughness ($R_t$) is the vertical distance between the highest and lowest points in the evaluated length/area and describes the overall roughness of the surface. Root mean square (RMS) roughness ($R_q$) is the square root of the distribution of surface height and is considered to be more sensitive than the average roughness for large deviations from the mean line/plane and is also used in computing the skew and kurtosis parameters. Ten-points mean height roughness ($R_z$) is the difference in height between the average of five highest peaks and five lowest valleys in the evaluation profile/surface and is more sensitive to occasional high peaks or deep valleys than $R_a$. Roughness skewness ($R_{sk}$) is used to measure the symmetry of the variations of a profile/surface about the mean line/plane and is more sensitive to occasional deep valleys or high peaks. Usually, $R_{sk}$ is used to distinguish two profiles of the same $R_a$ or $R_q$ values but of different shapes. Roughness kurtosis ($R_{ku}$) is used to measure the distribution of the spikes above and below the mean line/plane.

## Results and Discussion

The microstructure, such as the grain size and the surface roughness, is one of the key parameters determining the electrical properties of high dielectric constant thin films [10]. The electrical properties of BST thin films are closely linked to the microstructure of the films such as grain size, cracks, pinholes and roughness [11]. Hence, if the grain size of the BST thin films is large, the dielectric constant may be similar to that of the bulk BST [12].

Conventional Metal-Ferroelectric Metal (MFS) structures have many problems such as difficulty in depositing ferroelectric thin films directly on silicon, high trap densities and diffusion of elements into silicon. However, incorporating MFS structures in standard CMOS processes will benefit from the usage of Si-substrates and plethora of established techniques for reduced fabrication cost. A possible solution for these problems is to use a buffer layer between the ferroelectric thin film and silicon [13]. $SiO_2$ layer has been used as the buffer in this research. Fig. 1 shows the cross-sectional view of BST80 film, 446.8 nm in thickness.

Fig. 2 shows the three-dimensional AFM micrographs of the surface of BST50, BST70 and BST80 single layer films with 160.8 nm thickness. The micrographs reveal that the films do not show continuous long trenches or blotches, which are indicative of a crack free and pinhole-free surface.

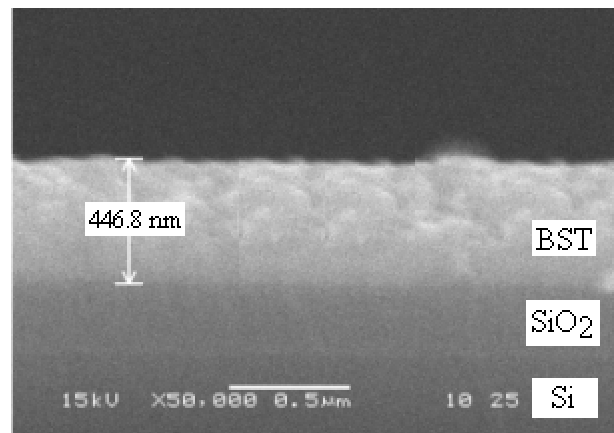


FIG. 1. SEM micrograph of the cross-section of BST80 film deposited on $SiO_2$/Si substrate.

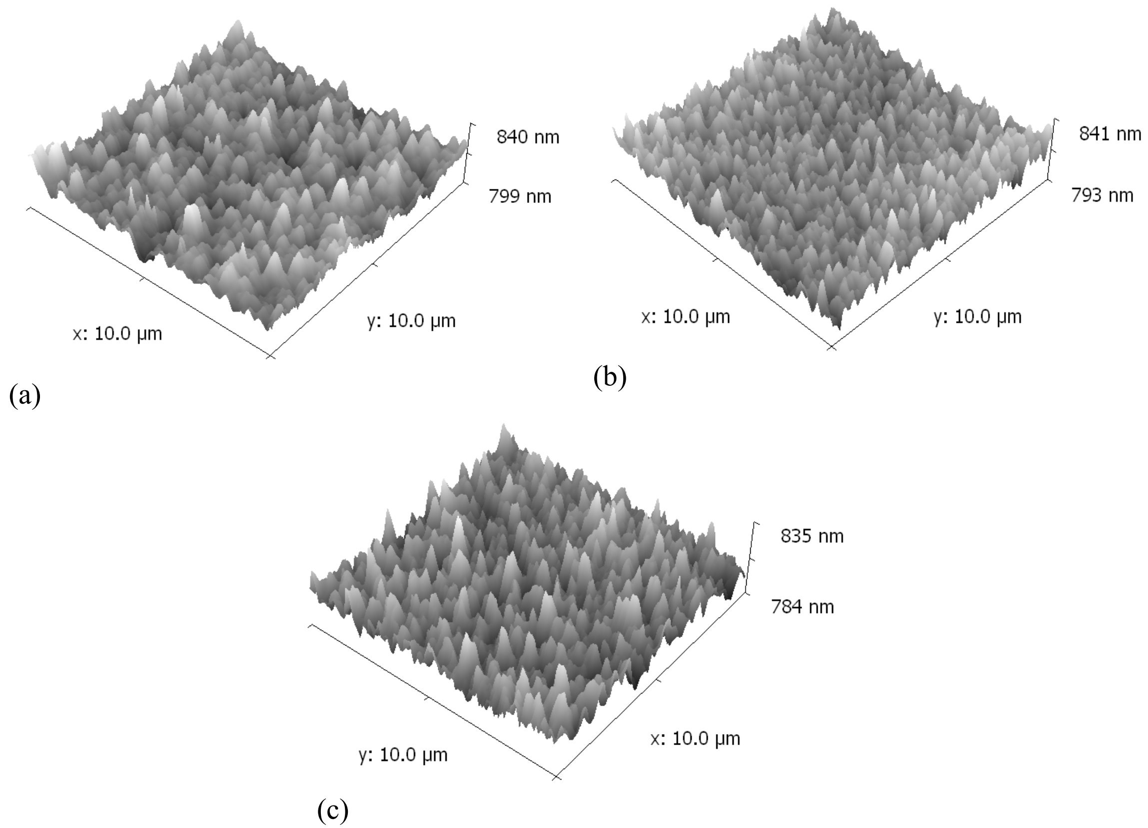


FIG. 2. Three dimensional AMF micrograph for a) BST50, b) BST70 and BST80 thin films with 160.8 nm thickness.

The variations of the root mean square roughness ($R_q$) of the BST50, BST70 and BST80 films as a function of the film thickness are shown in Fig. 3. The RMS roughness increases with film thickness almost linearly, as well as with increasing Ba content. The increase in $R_q$ for high Ba content films is due to the size difference between $Ba^{2+}$ ions (*r* = 0.135 nm) and $Sr^{2+}$ ions (*r* = 0.113 nm). The rest of the roughness parameters of the tested samples is summarized in Table 2.

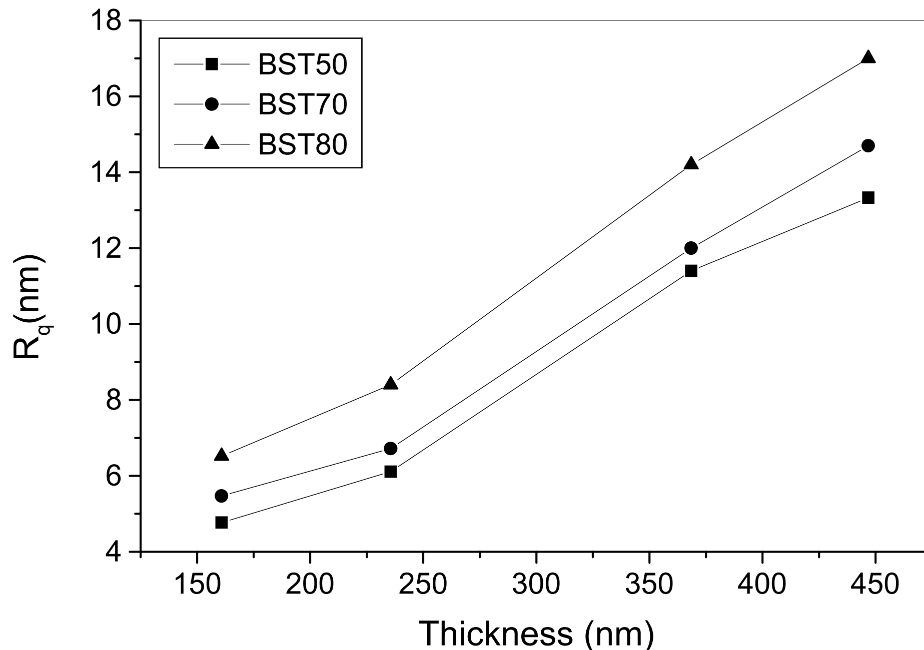


FIG. 3. Variations of the root mean square roughness for different thicknesses of BST films (BST50, BST70 and BST80).

Table 2 illustrates that the variations of the average roughness values ($R_a$) and ten-point mean height ($R_z$) values have the same trend as the variations of RMS roughness ($R_q$) values for all molar ratios and thicknesses. Maximum peak to valley height ($R_t$) is also considered a very important parameter because it gives a good description of the overall roughness of the surface. The results from the Table show that $R_t$ is high for BST70 and BST80 compared to BST50, which means that the surface roughness increases with Ba content, indicating that as Ba content increases bigger individual unit cells lead to larger clumps of grains. $R_t$ also shows notable increments as the film thickness of BST50 increases. BST70 and BST80 samples lack this trend for films with three and four layers. The Table also shows that for high values of $R_t$, $R_z$ is also high due to the strong dependence of $R_z$ on the peak heights / valley depths. $R_z$ is mathematically given by the following formula [5]:

$$R_z = \frac{1}{n}\left(\sum_{i=1}^{n} P_i - \sum_{i=1}^{n} V_i\right) \quad (1)$$

where n is the number of sampling points along the assessment length, which is 5 in this study, $P_i$ is the height of the i-th peak and $V_i$ is the depth of the i-th valley with respect to the line profile.

In addition, $R_q$ values for all the samples are higher than $R_a$ values, which can be mathematically explained according to the following equations [5].

$$R_a = \frac{1}{L}\int_0^L |y(x)|.\ dx \quad (2)$$

$$R_q = \sqrt{\frac{1}{L}\int_0^L \left|\left(y(x)\right)^2\right|.\ dx} \quad (3)$$

where L is the length of the profile on the x-axis used for measurement and y(x) is the variation of the height from the profile line for each data point.

TABLE 2. The roughness parameters of BST50, BST70 and BST80 at different thicknesses.

| Sample | Thickness (nm) | $R_a$ (nm) | $R_t$ (nm) | $R_q$ (nm) | $R_z$ (nm) | $R_{sk}$ | $R_{ku}$ |
|---|---|---|---|---|---|---|---|
| BST50 | 160.8 | 3.65 | 27.6 | 4.77 | 16.43 | 0.35 | 3.93 |
| | 235.6 | 4.65 | 38.9 | 6.11 | 20.94 | -0.25 | 3.19 |
| | 368.5 | 9 | 59.4 | 11.4 | 34.69 | 0.19 | 3.60 |
| | 446.8 | 10.59 | 65.4 | 13.33 | 43.8 | 0.43 | 3.08 |
| BST70 | 160.8 | 4.33 | 29.6 | 5.47 | 17.94 | 0.14 | 3.21 |
| | 235.6 | 5.25 | 36.81 | 6.72 | 21.41 | 0.25 | 3.57 |
| | 368.5 | 9.16 | 124 | 12 | 48.4 | 1.37 | 11.17 |
| | 446.8 | 11.2 | 95.4 | 14.7 | 56.2 | 0.21 | 5.85 |
| BST80 | 160.8 | 5.14 | 32.5 | 6.52 | 22.1 | 0.46 | 3.36 |
| | 235.6 | 6.6 | 45.1 | 8.4 | 24.2 | 0.325 | 3.38 |
| | 368.5 | 9.7 | 116.7 | 14.2 | 57.2 | -0.05 | 8.77 |
| | 446.8 | 13.4 | 92.41 | 17 | 58.47 | 0.29 | 3.34 |

In Table 2, negative values of the skewness indicate that the valleys are dominant over the scanned area and positive values show that the peaks are dominant on the surface. Continued negative values would indicate cracks, representative of valleys. The distribution of positive and negative values indicates the existence of protruding grains. For kurtosis, an $R_{ku}$ below three shows that the distribution over the scanned area has relatively few high peaks and low valleys, which means a bumpy surface. When $R_{ku}$ is more than three, the distribution will have relatively higher numbers of high peaks and low valleys, characteristic of a spiky surface [5]. The results of skewness and kurtosis show that the BST surface generally is spiky with peaks being dominant. Films with high $R_{ku}$ values have high $R_t$ and $R_z$ values as well. This is due to the strong relation between these parameters, where $R_{ku}$ is, mathematically, directly related to the peak heights and valley depths according to the following formula [5].

$$R_{ku} = \frac{1}{NR_q^4}\left(\sum_{i=1}^{N} Y_i^4\right) \quad (4)$$

where $R_q$ is the RMS roughness parameter and $Y_i$ is the height of the profile at point number i.

Fig. 4 shows a two-dimensional AFM micrograph with 500×500 $nm^2$ scanned area for different thicknesses of BST50, BST70 and BST80 films. The grain distribution is uniform for all three types. The values of the grain sizes for BST50, BST70 and BST80 films are plotted against film thickness, as illustrated in Fig. 5. It is clearly seen that the grain size increases with increasing Ba content and film thickness. The increase of the grain size in high Ba content films is due to the fact that Ba has a larger ionic radius which causes a larger crystalline unit cell, which in turn causes larger clumps of unit cells or grains.

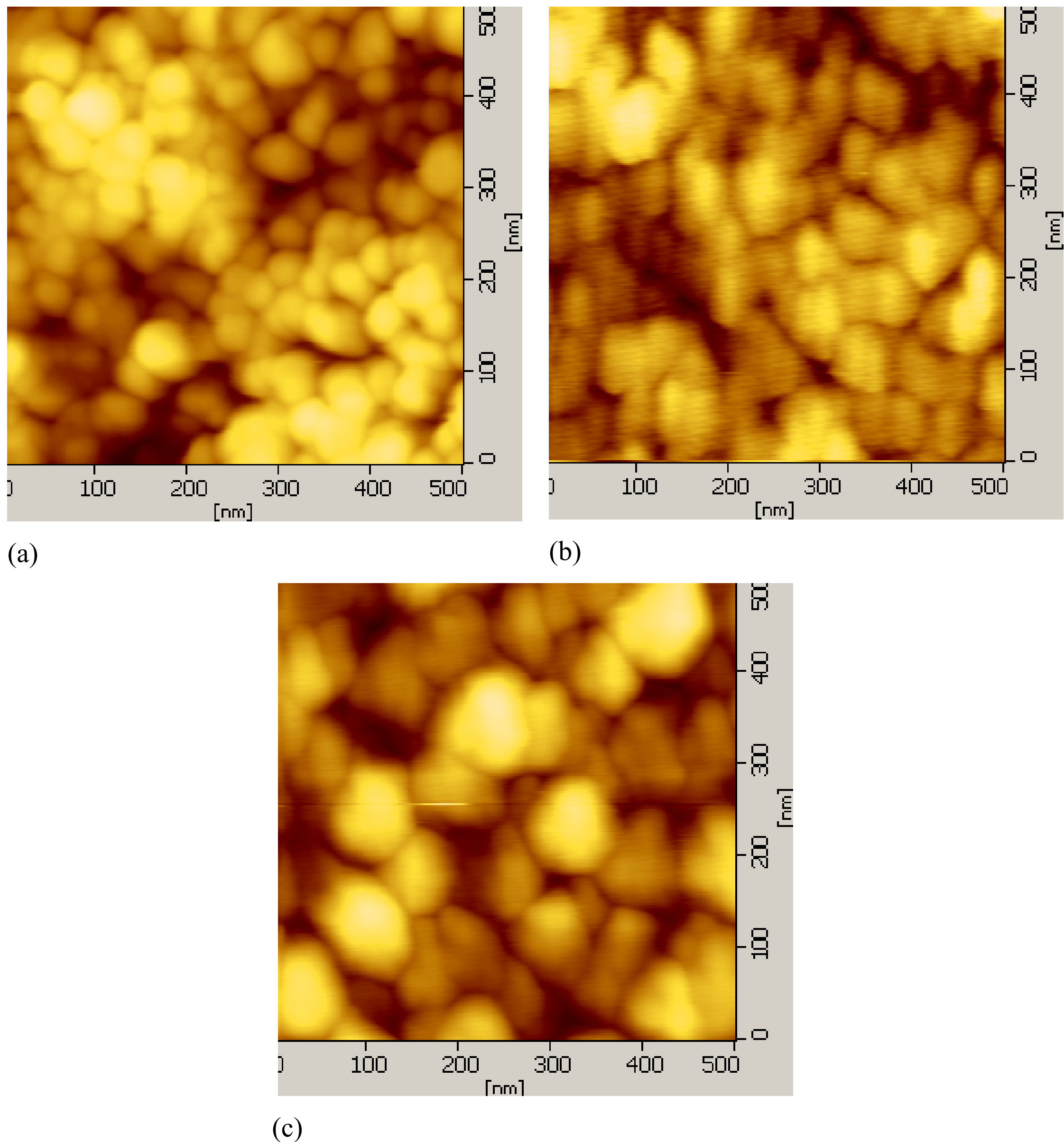


FIG. 4. Two-dimensional AFM micrograph of a) BST50, b) BST70 and c) BST80 films showing the distribution of the grains.

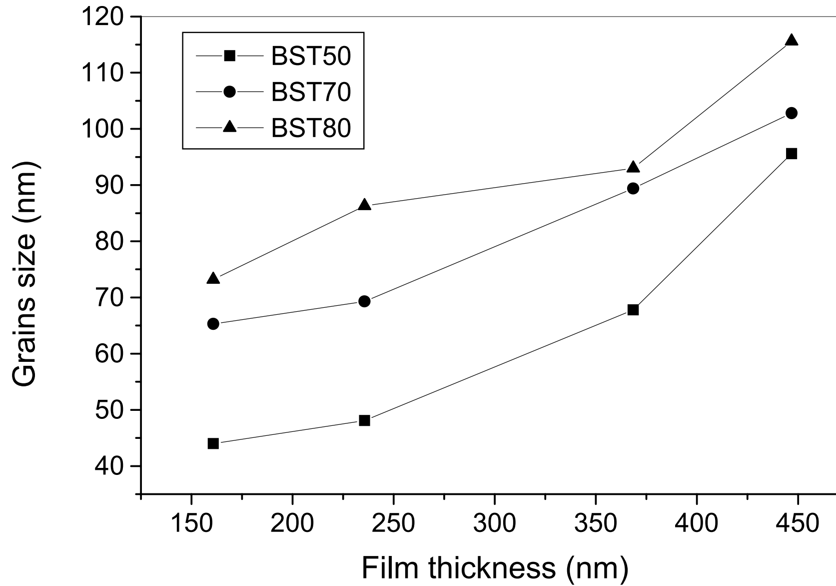


FIG. 5. The variation of grain size with film thickness for different Ba-Sr molar contents.

Adding $Sr^{2+}$ ions to BST changes the unit cell volume, where Strontium ions are introduced at the A site of the perovskite matrix and enter substitutionally into the $Ba^{2+}$ ion sites [14]. The small size of $Sr^{2+}$ ions causes the unit cell to become smaller. This substitution of ions will also affect the dielectric and electrical properties of BST. As the number of $Sr^{2+}$ ions increase in the lattice, a smaller unit cell will be obtained which leads to smaller grain growth during annealing. The bright grains appearing in the AFM images in Fig. 4 represent grains closer to the surface.

The increase in surface roughness and grain size with the increase in film thickness is due to grain growth during the deposition and annealing process of the layers. During deposition, the film is heated at 500 ˚C for 30 min after each layer, this temperature is enough to grow the BST grains, so the next layer deposition is carried out over films with established grain boundaries and the solution is randomly spread over all these grains, so bigger grains will be obtained after the heating and annealing of the new layer.

The results of the surface roughness and the grain size show that their values can be controlled by adjusting the Ba-Sr ratio and the number of layers deposited. Furthermore, changing the number of layers deposited has a more significant effect on grain size than that due to Ba-Sr ratio (for the same thickness).

## Conclusion

Multilayer Barium Strontium Titanate (BST) films with the molar formula $Ba_xSr_{1-x}TiO_3$ ($x$ = 0.5, 0.7 and 0.8) have been fabricated on $SiO_2$/Si substrates by sol-gel technique. The surface morphology and the grain size are characterized via Atomic Force Microscope (AFM). The results show that the sol-gel technique has a high efficiency in fabricating high quality BST thin films on $SiO_2$/Si substrates, as shown by the very dense, crack-free films formed with low surface roughness and possessing relatively large grain sizes. Generally, the surface roughness increases as Sr content decreases (1-x value), where the root mean square roughness increases from 4.95 nm to 6.9 nm for films of 160.8 nm thickness as Sr content decreases. The surface roughness also increases as the number of layers (film thickness) increases, for $x$ = 0.5, RMS roughness increases from 4.95 nm to 13.5 nm as the film thickness increases from 160.8 nm to 446.8 nm. A similar trend for surface roughness is obtained, for all x values, as is for grain size. The values of surface roughness and grain size can be controlled by adjusting the Ba-Sr ratio and the number of deposited layers. Surface roughness and grain size for all samples show a direct relation between each other where the surface roughness shows an increasing trend as the grain size increases. The BST surface is dominated by peaks with lots of high peaks and low valleys.

## References

[1]Hongwei, C., Chuanren, Y., Chunlin, F., Li, Z. and Zhiqiang, G., Appl. Surf. Sci. 252 (2006) 4171.

[2]Li, G., Yu, P. and Xiao, D., J. Electroceram. 21 (2008) 340.

[3]Cui, D., Lu, H., Wang, H. and Tao, H., Chin. Phys. Lett. 14 (1997) 134.

[4]Bałamucki, J., Czarnecki, P., Gotszalk, T. and Kowalski, Z.W., Phys. Chem. Sol. State. 8 (2007) 583.

[5]Gadelmawlaa, E.S., Kourab, M.M., Maksoudc, T.M.A., Elewaa, I.M. and Solimand, H.H., J. Mater. Process. Tech. 123 (2002) 133.

[6]Wysocka, K., Ulatowska, A., Bauer, J., Holowacz, I., Savu, B. and Stanciu, G., Optica Applicata. XXXVIII (2008) 130.

[7]Chunlin, F., Chuanren, Y., Hongwei, C., Liye, H. and Yingxin, W., Mater. Lett. 59 (2005) 330.

[8]Wencheng, H., Chuanren, Y., Wanli, Z. and Lin, Z., Integ. Ferroelect. 72 (2005) 1.

[9]Personal communications with Mr. David Necas to modify Gwyddion software to fit with SII nanotechnology Ins AFM images format.

[10]Ru-Bing, Z., Chun-Sheng, Y., Gui-Pu, D. and Jie, F., Mater. Res. Bull. 40 (2005) 1490.

[11]Mazon, T., Zaghete, M.A., Varela, J.A. and Longo, E., J. Eur. Ceram. Soc. 27 (2007) 3799.

[12]Qin, W.F., Xiong, J., Zhu, J., Tang, J.L., Jie, W.J., Wei, X.H., Zhang, Y. and Li, Y.R., J. Mater. Sci: Mater. Electron. 18 (2007) 973.

[13]Woo-Sik, K., Su-Min, H., Jun-Kyu, Y. and Hyung-Ho, P., Thin Solid Films, 398 –399 (2001) 663.

[14]Patil, D.R., Lokare, S.A., Devan, R.S., Chougule, S.S., Kanamadi, C.M., Kolekar, Y.D. and Chougule, B.K., Mater. Chem. Phys. 104 (2007) 254.